Proceedings of the 1993 IEEE/RSJ International Conference on Intelligent Robots and Systems Yokohama, Japan July 26-30, 1993

Screw Axis Measurement for Kinematic Calibration of the Sarcos Dextrous Arm

John M. Hollerbach, Lydia Giugovaz, Martin Buehler, and Yangming Xu

Biorobotics Laboratory, McGill University
3775 University St., Montreal, Quebec H3A 2B4

Abstract

A recently developed kinematic calibration technique for 6 degree-of-freedom (DOF) arms, the Jacobian measurement method, is generalized to include underconstrained and overconstrained arms. Using joint torque sensing and a wrist 6-axis force/torque sensor to measure the Jacobian, experimental results are presented for the first 5 DOFs of the Sarcos Dextrous Arm. Results are compared to two standard calibration methods, i.e., open loop calibration and circle point analysis. Measurements of endpoint position and orientation were obtained with the Optotrak and the Bird sensor, two commercial motion tracking systems.

1 Introduction

Recently, an alternative kinematic calibration approach was introduced that involves direct measurement of the Jacobian matrix [4]. The Jacobian matrix can be measured either by sensing joint torques and the corresponding endpoint forces and torques, or by sensing joint angle velocities and the corresponding endpoint linear and angular velocities. The kinematic parameters can then be extracted directly from the elements of the Jacobian, exactly and without iteration. Simulations were presented for a 6-DOF manipulator with a nominal PUMA 560 geometry. The Denavit-Hartenberg parameterization [5] was used along with modified Hayati parameters [7].

In this paper, we extend the Jacobian measurement method, originally developed for 6-DOF manipulators, to overconstrained manipulators (≤ 5 DOFs) and to redundant manipulators (≥ 7 DOFs). We then experimentally implement the method on the first 5 DOFs of the Sarcos Dextrous Arm [13, 12], by using joint torque sensing intrinsic to the arm's design and a six-axis force/torque sensor (Assurance Technology, Garner, North Carolina) at the endpoint. We compare the results to those obtained by applying two standard calibration techniques, open-loop kinematic calibration [1, 11] and circle point analysis (CPA) [14], using endpoint measurements obtained respectively with the Optotrak, a commercial optoelectronic motion tracking system (Northern Digital Inc., Waterloo, Ontario), and the Bird sensor, a magnetic motion tracking system (Ascension Technology, Burlington, Vermont).

In open-loop kinematic calibration, the manipulator is placed in a number of poses and the endpoint position and orientation are measured. Nonlinear optimization, usually the Levenberg-Marquardt algorithm, is performed to extract the kinematic parameters. The phrase *open-loop* refers to an endpoint which is positioned freely in space, in contrast to *closed-loop* methods where the endpoint is attached to the environment [2, 3].

Circle point analysis (CPA) is also a kind of open-loop method, but proceeds quite differently from the open-loop method just described. Each joint is moved alone; a linear optimization then fits a least squares plane to the data, followed by a nonlinear optimization which fits a circle in this plane. The plane gives the orientation of the joint axis, while the circle yields a point on this axis; thus the line in space for each joint axis is known. Different procedures have been proposed to extract the kinematic parameters from a knowledge of the joint axes [14, 17].

The Jacobian measurement method may be either open or closed loop, depending on the sensing. When endpoint force/torque sensing and joint torque sensing are used, the manipulator forms a closed loop. When endpoint linear and angular velocity and joint angle velocity are sensed, the manipulator is in an open loop.

There is a strong relation between CPA and the Jacobian measurement method, because both involve measurement of the screw coordinates of the joint axes. In CPA, the screw axes are obtained one at a time by individual joint motion. In the Jacobian measurement method, the screw axes are deduced together because the Jacobian as a whole is calculated from the measurements by matrix inversion. Once the screw axes have been obtained, whether from CPA or the Jacobian measurement method, the same methods can be applied to extract the kinematic parameters from the screw axes. The method that we proposed in [4] is most similar to Sklar's method [14, 16].

Since CPA and the Jacobian measurement method have this strong relation, it may be worth coining a new phrase to describe a more general class of calibration methods that includes them both. We suggest *screw axis measurement*. Other screw axis measurement methods besides these two are conceivable, and so this phrase may have additional utility.

In the following, we first extend the Jacobian measurement method to overconstrained 5-DOF arms, then to redundant 7-DOF arms. The experimental setup involving the Sarcos Dextrous Arm is then described, and calibration results are presented.

2 Jacobian Measurement Method

For brevity, we will describe only the approach using joint torque sensing and wrist force/torque sensing. Extensions to velocity sensing are straightforward, and for the 6-DOF case are described in [4]. The basis for the approach is the well-known static relation:

$$\tau^i = \mathbf{J}^T \mathbf{w}^i + \mathbf{g} \tag{1}$$

where τ^i is the vector of joint torques, $\mathbf{w}^i$ is the wrench, $\mathbf{g}$ is the gravity torque vector, and the superscript i refers to the ith measurement point.

The Jacobian $\mathbf{J}$ is not superscripted because the manipulator position is always the same in this method, and is related to the screw Jacobian matrix $\mathbf{J}_s$ by the relation:

$$\mathbf{J} = \begin{bmatrix} \mathbf{0}_3 & \mathbf{I}_3 \\ \mathbf{I}_3 & \mathbf{0}_3 \end{bmatrix} \mathbf{J}_s = \mathbf{A}\mathbf{J}_s \tag{2}$$

where $\mathbf{0}_3$ is the 3-by-3 zero matrix, $\mathbf{I}_3$ is the 3-by-3 identity matrix. For an n-joint manipulator, $\mathbf{J}_s$ has the form [2]:

$$\mathbf{J}_s = \begin{bmatrix} \mathbf{z}_0 & \cdots & \mathbf{z}_{n-1} \\ \mathbf{z}_0 \times \mathbf{b}_1 & \cdots & \mathbf{z}_{n-1} \times \mathbf{b}_n \end{bmatrix} \tag{3}$$

where $\mathbf{z}_{j-1}$ is the rotation axis for joint j, and $\mathbf{b}_j$ is any vector from axis $\mathbf{z}_{j-1}$ to the endpoint.

0-7803-0823-9/93/$3.00 (C) 1993 IEEE

2.1 Fully Constrained Manipulators

For 6-DOF manipulators, we estimate $\mathbf{J}$ by exerting six joint torques τ^i, $i = 1, \ldots, 6$, that yield independent endpoint wrenches $\mathbf{w}^i$. The bias due to gravity torques is eliminated by exerting both positive τ^i and negative $-\tau^i$ torques for each torque vector application, then subtracting the corresponding static equations (1):

$$\tau^i = \mathbf{J}^T \mathbf{w}_+^i + \mathbf{g} \qquad (4)$$

$$-\tau^i = \mathbf{J}^T \mathbf{w}_-^i + \mathbf{g} \qquad (5)$$

where $\mathbf{w}_+^i$ and $\mathbf{w}_-^i$ are the wrenches resulting from the positive and negative torque applications respectively. Subtracting these equations eliminates gravity:

$$2\tau^i = \mathbf{J}^T \Delta\mathbf{w}^i \qquad (6)$$

where $\Delta\mathbf{w}^i = \mathbf{w}_+^i - \mathbf{w}_-^i$. From the six differential measurements (6), form the matrices $\mathbf{T} = (2\tau^1, \ldots, 2\tau^6)$ and $\mathbf{W} = (\Delta\mathbf{w}^1, \ldots, \Delta\mathbf{w}^6)$. Then

$$\mathbf{T} = \mathbf{J}^T \mathbf{W} \qquad (7)$$

$$\mathbf{J}^T = \mathbf{T}\mathbf{W}^{-1} \qquad (8)$$

where the measured Jacobian (8) is obtained from (7) by inverting $\mathbf{W}$.

To generate an independent wrench set, the manipulator must not be in a singular position. A singularity may be detected by checking the rank of the generated wrenches $\mathbf{W}$. If singular, a new position and attachment point to the environment would have to be sought that is not at a singularity. When the position is not singular, an independent wrench set may be obtained by generating torque at one joint at a time. Let $\tau^i = \mathbf{e}^i$, where the jth component of e^i_j is 1 if $i = j$ and 0 otherwise. Then from (6)

$$\Delta\mathbf{w}^i = \mathbf{J}^{-T}(2\mathbf{e}^i) \qquad (9)$$

As long as $\mathbf{J}$ is invertible, the resulting wrenches are independent but not usually orthogonal.

2.2 Overconstrained Manipulators

When there are 5 or fewer DOFs, the endpoint wrenches generated by the joint torques do not span the full six-dimensional space. Hence it is not possible to use the exact procedure above, which requires an invertible $\mathbf{W}$. Because experiments will be presented later for a manipulator with 5 DOFs, we restrict the following discussion to 5-DOF arms. From (6), the pseudoinverse solution for $\Delta\mathbf{w}^i$ is:

$$\Delta\mathbf{w}^i = (\mathbf{J}^T)^* 2\tau^i + (\mathbf{I}_6 - (\mathbf{J}^T)^*\mathbf{J})\mathbf{v} \qquad (10)$$

where $(\mathbf{J}^T)^* = \mathbf{J}(\mathbf{J}^T\mathbf{J})^{-1}$ is the pseudoinverse of $\mathbf{J}^T$, $\mathbf{I}_6$ is the 6-by-6 identity matrix, and $\mathbf{v}$ is an arbitrary wrench. The second term on the right side represents a vector in the null space of $\mathbf{J}^T$, i.e., a wrench which generates no joint torques. The first term on the right represents the endpoint wrenches which can actively be generated by the manipulator. Since in our scenario the manipulator is the active source of wrench generation (once gravity has been accounted for), the second term on the right side is zero. Thus the measured wrenches will correspond only to those actively generated by the joint torques.

Five independent measurements need to be generated, for example, by the single-joint actuation method described above. Combining these five independent measurements, (10) becomes

$$\mathbf{W} = (\mathbf{J}^T)^*\mathbf{T} \qquad (11)$$

where $\mathbf{W}$ consists of the 5 independent wrenches that are actually produced from the joint torques.

The solution for $\mathbf{J}$ can now be obtained by taking the transpose of (7) and using the pseudoinverse of $\mathbf{W}^T$:

$$\mathbf{J} = (\mathbf{W}^T)^*\mathbf{T}^T = \mathbf{W}(\mathbf{W}^T\mathbf{W})^{-1}\mathbf{T}^T \qquad (12)$$

That (12) yields the correct solution may be verified by substituting (11).

2.3 Underconstrained Manipulators

With rigid attachment of the endpoint to the environment, a redundant manipulator with 7 DOFs will in general form a mobile closed kinematic chain with 1 DOF. The main difficulty in extending the Jacobian measurement method to redundant manipulators is to generate a set of joint torques which do not result in an internal motion of the mobile closed chain. Borrowing a technique developed in [6] for redundancy resolution, we note that six components of joint torque can be considered independent while the seventh is dependent. Without loss of generality, assume τ_7 is the dependent torque. If joint 7 is immobile during the self motion, we may rearrange the Jacobian to place a mobile joint in position 7. The mobility of joints may be discovered experimentally, by finding a joint that drives the chain when other joint torques are servoed to 0.

First we need to counteract gravity for an arm to hold an arbitrary posture. This can be done, for example, by servo action on joint 7 to discover the required joint torque. Let τ_0 be this applied torque vector and $\mathbf{w}_0$ the resulting endpoint wrench. We can again eliminate the effect of gravity by a difference method, this time subtracting the following bias equation from each reading:

$$\tau_0 = \mathbf{J}^T\mathbf{w}_0 + \mathbf{g} \qquad (13)$$

Next define a reduced torque vector $\bar{\tau}^i$ from the first six joint torque components of τ^i. Apply the method in Section 2.1 for fully constrained manipulators to generate six joint torques $\bar{\tau}^i$. For each torque application $\bar{\tau}^i$, servo joint 7 to remain stationary and read the resulting joint torque τ_7^i. Then read the resulting wrench $\mathbf{w}_i$. The static force-torque relation may be written as:

$$\tau^i = \begin{bmatrix} \bar{\tau}^i \\ \tau_7^i \end{bmatrix} = \mathbf{J}^T\mathbf{w}^i + \mathbf{g} \qquad (14)$$

Subtracting the bias torque (13) to eliminate gravity,

$$\tau^i - \tau_0 = \mathbf{J}^T(\mathbf{w}^i - \mathbf{w}_0) \qquad (15)$$

The 6-by-7 Jacobian is then found straightforwardly using the procedures of Section 2.1.

3 Methods

At the time of the experiments, our Sarcos Dextrous Arm was configured with the first 5 arm joints: a roll-pitch-roll spherical shoulder joint, a rotary elbow joint, and a roll forearm joint. Hence for the Jacobian measurement method, the overconstrained method discussed in Section 2.2 was implemented.

Each joint of our Sarcos Dextrous Arm is sensed by two different joint angle sensors, 400,000 count optical encoders and Rotary Variable Differential Transducers (RVDTs). In this preliminary experimental study, readings from the Arm's standard RVDTs were employed for both the Open-loop and CPA method. Their analog signals are converted by 12-bit ADCs. The manufacturer specifies a linearity of 2% of full scale of a best fit straight line. In addition we observe a noise level of 2 bits.

The D-H parameters are employed and derived, namely for joint j:

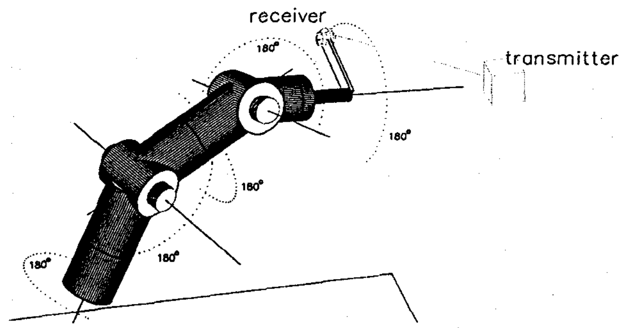

Figure 1: Diagram of Sarcos Dextrous Arm for CPA calibration.

a_j is the distance along axis $\mathbf{x}_j$ from rotation axis $\mathbf{z}_{j-1}$ to rotation axis $\mathbf{z}_j$.

s_j is the distance along axis $\mathbf{z}_{j-1}$ from axes $\mathbf{x}_{j-1}$ to $\mathbf{x}_j$.

α_j is the skew angle about $\mathbf{x}_j$ from $\mathbf{z}_{j-1}$ to $\mathbf{z}_j$.

θ_j^{off} is the joint angle offset.

The D-H parameters derived from the manufacturer's specifications are listed in Table 1, and are used as a point of reference for the experimental results.

3.1 Open-Loop Method

The procedure presented in [11] was implemented using the OPTOTRAK 3020, which has a stated accuracy of 0.1-0.15 mm in a 1 m^3 workspace. A calibration frame was attached to the endpoint of the Sarcos Dextrous Arm, and six IREDs (infrared light emitting diodes) were attached in the shape of a rectangle.

The calibration frame was placed by the manipulator into 250 poses, carefully chosen to be in view of the camera system. At each pose, Optotrak IREDS and joint angle sensors were sampled and averaged for 200 times.

From the six IREDs, the position and orientation of the calibration frame were derived at each pose and compared to those predicted from the nominal parameters to yield the position and orientation errors. A standard iterative least squares method was employed to derive the D-H parameters, including extra parameters to locate the calibration frame in the last link and the base of the robot relative to the camera coordinate system.

3.2 Circle Point Analysis

The procedure presented in [14, 16] was implemented using an Ascension Technology Bird sensor, which has a stated accuracy of 2.5 mm in translation and 0.5° rotation in a spherical workspace of 1.2 m diameter. Each joint of the arm was rotated by steps throughout its entire range. At each pose the position and orientation of the Bird sensor attached to the end-effector was sampled and averaged 25 times.

Theoretically, the resulting trajectory is a circle constrained to a plane. In practice, we first fit a plane to the experimental data, project the data points onto this plane, and then fit a circle to the projected data. The resulting normal to the plane through the center of the circle uniquely determines a line which is the *screw axis* of the rotating joint. With all the screw axes available, the arm's D-H parameters can be determined immediately exploiting simple geometric relationships.

3.3 Jacobian Measurement Method

In this method the robot arm's motion is completely constrained. To this end, a fixture was made which rigidly attached the arm's last link via the force torque sensor to the robot mounting table. Simulations were performed to find a pose for which the numerical calibration procedure is well conditioned. To cancel out the gravity terms, torques of opposite sign where generated at each joint. The resulting joint torques and wrenches can then be used to calculate the manipulator Jacobian.

For joint torque measurement, we employ the Sarcos Dextrous Arm's intrinsic joint torque sensors, which have a stated resolution of 1 part in 2000. The torque sensors were calibrated by the manufacturer, and we assumed this calibration level to proceed. The measurement noise in the joint torque sensors is about 2 counts or 0.1% full scale.

An Assurance Technology FT 500/3000 model six-axis force/torque sensor was employed as the external wrench sensor. Its full scale of 500 lbs for force and 3000 in-lbs for torque was selected to accommodate the maximum wrenches exerted by the arm, and thus maximize the measurement accuracy. The manufacturer specifies an accuracy for the force/torque sensor of around 1%.

4 Experimental Results

The results from the open-loop method, the CPA, and the Jacobian measurement method are presented in Tables 2, 3, and 4 respectively. The terms that are noted as n/a are not considered as they are dependent on the fixtures of the base and of the end-effector and are not part of the arm's D-H parameter set.

In comparing the calibrated parameters to the manufacturer's parameters, we use the statistical root mean square (RMS) measure. For the length components, the RMS error ψ_l is defined as:

$$\psi_l = \sqrt{1/2N \sum_{j=1}^{N} (a_j - a_j^m)^2 + (s_j - s_j^m)^2} \tag{16}$$

where a_j^m and s_j^m are the manufacturer's parameters (Table 1), a_j and s_j are the parameters calibrated by one of the three methods (Tables 2 - 4), and N is the number of joints. For the angle components, the RMS error ψ_a is defined similarly:

$$\psi_a = \sqrt{1/2N \sum_{j=1}^{N} (\alpha_j - \alpha_j^m)^2 + (\theta_j^{off} - \theta_j^{off,m})^2} \tag{17}$$

The statistical errors are summarized in Table 5.

5 Discussion

Statistical analysis (Table 5) shows that the open-loop method using the Optotrak yielded the most accurate results, which was expected. The RMS error in the length parameters ψ_l was 2 mm while that in the angle parameters ψ_a was 0.3 degrees. These are reasonable results, considering the lack of precision in the RVDT angle sensors. In the future, we plan to redo the experiments using the substantially more accurate digital encoders.

The results from CPA using the Bird sensor were the least accurate, with a ψ_l of 45 mm and ψ_a of 1.2 degrees. The length parameter errors using the Bird sensor were about 20 times worse than for the Optotrak, which is roughly proportional to the price ratio of the two systems.

The Jacobian measurement method using joint torque sensing and an Assurance Technology wrist force/torque sensor yielded a ψ_l of 17 mm and a ψ_a of 0.4 degrees.

j	a_j^m (m)	s_j^m (m)	α_j^m (deg)	$\theta_j^{off,m}$ (deg)
1	0.000	n/a	90.0	n/a
2	0.000	0.000	-90.0	135.0
3	0.000	0.355	90.0	-180.0
4	0.000	0.000	-90.0	135.0
5	n/a	0.235	n/a	90.0

Table 1: D-H parameters according to manufacturer's specifications.

j	a_j (m)	s_j (m)	α_j (deg)	θ_j^{off} (deg)
1	0.001	n/a	90.0	-89.8
2	0.000	0.003	-89.9	135.9
3	0.001	0.355	90.0	-180.0
4	0.000	0.003	-89.8	135.0
5	n/a	0.232	n/a	90.2

Table 2: D-H parameters derived from open-loop method.

j	a_j (m)	s_j (m)	α_j (deg)	θ_j^{off} (deg)
1	0.046	0.034	88.1	-90.8
2	-0.012	0.060	-88.6	134.6
3	-0.009	0.350	88.0	-179.8
4	0.005	0.091	-89.4	134.8
5	0.013	n/a	n/a	n/a

Table 3: D-H parameters derived from CPA.

j	a_j (m)	s_j (m)	α_j (deg)	θ_j^{off} (deg)
1	0.005	n/a	89.9	n/a
2	0.030	0.003	-89.6	134.9
3	0.028	0.343	90.0	-179.9
4	0.017	0.003	-90.0	135.3
5	0.001	0.220	n/a	91.1

Table 4: D-H parameters derived from Jacobian measurement method.

Method	ψ_l (m)	ψ_a (deg)
Open-loop	0.002	0.3
CPA	0.045	1.2
JMM	0.017	0.4

Table 5: RMS errors relative to the manufacturer's specifications for the D-H length parameters (ψ_l) and for the D-H angle parameters (ψ_a).

The main limitation in this implementation of the Jacobian measurement method was the accuracy of the wrist force/torque sensor. While the stated accuracy is 1%, the actual accuracy is likely to be worse because of nonlinear coupling among force directions. Hirose et al. (1990) have shown that such nonlinear coupling can degrade the accuracy for sensors initially rated at 0.2% down to 3%, and have proposed a compensation method that reduces the error below 1%. If only on-axis wrenches are generated, wrist force sensors are at their most accurate. For this purpose, it is possible to recast this method into a multi-step procedure, first generating a rough model with the method presented, then using this model to generate approximately on-axis wrench components, and finally refining these components through a small experimental search procedure to produce on-axis wrenches. Future force sensor developments should also result in more accurate sensors, such as the optically-based force sensors in [8] or force sensors based on magnetic levitation, which have no coupling.

For CPA, one limitation in our experimental results was deflections in stationary joints during motion of the joint to be calibrated, up to 1 degree. This was due to inadequate stiffness in the PD controller. We will implement a PID controller to compensate for these deflection errors.

6 Conclusion

The primary purpose of this paper was an experimental implementation of the Jacobian measurement method, using joint torque sensing coupled with wrist force/torque sensing. This method was implemented on the Sarcos Dextrous Arm, which has joint torque sensing at every joint. Because our arm was configured for 5 DOFs, we extended our original approach [4], developed for 6-DOF arms, to overconstrained arms with less than 6 DOFs. The main issue in the extension was that 6 independent wrenches could not be generated, and the proposed solution involved the pseudoinverse of the wrench matrix $\mathbf{W}$. Our arm is currently configured as a redundant 7-DOF arm, and so the method was also extended to redundant arms. The main issue in this extension is to prevent internal motion of the manipulator when joint torques are exerted, and a solution was devised in which one of the joint torques is treated as a dependent variable.

We also showed how the Jacobian measurement method is related to another calibration method, circle point analysis (CPA). Both methods determine the screw axes of the joints, and we suggested the term *screw axis measurement* to encompass these two and other conceivable approaches.

The experimental results of Jacobian measurement method were compared to experimental results using the open-loop method and also CPA. For the open-loop method, the Optotrak system was employed to provide high-accuracy position measurements of the endpoint. For CPA, we decided to employ the much less expensive Bird sensor for interest to see how well calibration could be performed. For both open-loop and CPA method, the RVDT sensors were used to provide joint-angle measurements. Baseline results were chosen to be the manufacturer's specifications.

These results indicate that at the moment the Jacobian measurement method using force and torque sensing is suitable for coarse calibration, but not for high-accuracy parameter determination. One use for the method is that the frame of the wrist force/torque sensor with regard to the end link can be determined. Another use is to check, or determine an initial value for the joint angle offset, which in many manipulators has to be recalibrated frequently.

Acknowledgements

Support for this research was provided by the Natural Sciences and Engineering Research Council (NSERC) Network Centers of Excellence Institute for Robotics and Intelligent Systems (IRIS). Personal support for JMH and MB was provided by the NSERC/Canadian Institute for Advanced Research (CIAR) Industrial Chair in Robotics. We acknowledge the contribution of Daniel Bunyan.

References

[1] C.H. An, C.G. Atkeson, and J.M. Hollerbach, *Model-Based Control of a Robot Manipulator.* Cambridge, MA: MIT Press, 1988.

[2] D.J. Bennett and J.M. Hollerbach, "Autonomous calibration of single-loop closed kinematic chains formed by manipulators with passive endpoint constraints," *IEEE Trans. Robotics and Automation*, vol. 7, pp. 597-606, 1991.

[3] D.J. Bennett, J.M. Hollerbach, and D. Geiger, "Autonomous robot calibration for hand-eye coordination," *Intl. J. Robotics Research*, vol. 10, pp. 550-559, 1991.

[4] D.J. Bennett, J.M. Hollerbach, and P.D. Henri, "Kinematic calibration by direct estimation of the Jacobian matrix," in *IEEE Intl. Conf. Robotics and Automation*, Nice, pp. 351-357, May 10-15, 1992.

[5] J. Denavit and R.S. Hartenberg, "A kinematic notation for lower pair mechanisms based on matrices," *J. Applied Mechanics*, vol. 22, pp. 215-221, 1955.

[6] R.V. Dubey, J.A. Euler, and S.M. Babcock, "Real-time implementation of an optimization scheme for seven-degree-of-freedom redundant manipulators," *IEEE Trans. Robotics and Automation*, vol. 7, pp. 579-588, 1991.

[7] S.A. Hayati and M. Mirmirani, "Improving the absolute positioning accuracy of robot manipulators," *J. Robotic Systems*, vol. 2, pp. 397-413, 1985.

[8] Hirose, S., and Yoneda, K., "Robotic sensors with photodetecting technology," in *Proc. Intl. Symp. Industrial Robots*, Tokyo, pp. 271-278, Oct. 4-6, 1989.

[9] S. Hirose and K. Yoneda, "Development of optical 6-axial force sensor and its signal calibration considering non-linear interference," in *Proc. IEEE Intl. Conf. Robotics & Automation*, Cincinnati, pp. 46-53, May 13-18, 1990.

[10] J.M. Hollerbach, "A review of kinematic calibration," *The Robotics Review 1*, edited by O. Khatib, J.J. Craig, and T. Lozano-Perez. Cambridge, MA: MIT Press, pp. 207-242, 1989.

[11] J.M. Hollerbach and D.J. Bennett, "Automatic kinematic calibration using a motion tracking system," *Robotics Research: the Fourth International Symposium*, edited by R. Bolles and B. Roth. Cambridge, MA: MIT Press, pp. 191-198, 1988.

[12] S.C. Jacobsen, F.M. Smith, D.K. Backman, and E.K. Iversen, "High performance, high dexterity, force reflective teleoperator II," in *ANS Topical Meeting on Robotics and Remote Systems*, Albuquerque, NM, Feb. 24-27, 1991.

[13] S.C. Jacobsen, F.M. Smith, E.K. Iversen, and D.K. Backman, "High performance, high dexterity, force reflective teleoperator," in *Proc. 38th Conf. Remote Systems Technology*, Washington, DC, Nov., 1990.

[14] B.W. Mooring, Z.S. Roth, and M.R. Driels, *Fundamentals of Manipulator Calibration.* NY: Wiley Interscience, 1991.

[15] Y. Nakamura, Kinematical Studies on the Trajectory Control of Robot Manipulators, Ph.D. Thesis, Kyoto Univ., June, 1985.

[16] M.E. Sklar, "Geometric calibration of industrial manipulators by circle point analysis," in *Proc. 2nd Conf. on Recent Advances in Robotics*, FAU, Boca Raton, FL, pp. 178-202, May 18-19, 1989.

[17] H.W. Stone, *Kinematic Modeling, Identification, and Control of Robotic Manipulators.* Boston: Kluwer Academic Publ., 1987.